The EMBO Journal (2004) 23, 1166–1177 | © 2004 European Molecular Biology Organization | All Rights Reserved 0261-4189/04
www.embojournal.org

THE EMBO JOURNAL

Functions of eIF3 downstream of 48S assembly impact AUG recognition and *GCN4* translational control

Klaus H Nielsen, Béla Szamecz, Leoš Valášek, Antonina Jivotovskaya, Byung-Sik Shin and Alan G Hinnebusch*

Laboratory of Gene Regulation and Development, National Institute of Child Health and Human Development, Bethesda, MD, USA

The binding of eIF2–GTP–tRNA$_i^{Met}$ ternary complex (TC) to 40S subunits is impaired in yeast *prt1-1* (eIF3b) mutant extracts, but evidence is lacking that TC recruitment is a critical function of eIF3 *in vivo*. If TC binding was rate-limiting in *prt1-1* cells, overexpressing TC should suppress the temperature-sensitive phenotype and *GCN4* translation should be strongly derepressed in this mutant, but neither was observed. Rather, *GCN4* translation is noninducible in *prt1-1* cells, and genetic analysis indicates defective ribosomal scanning between the upstream open reading frames that mediate translational control. *prt1-1* cells also show reduced utilization of a near-cognate start codon, implicating eIF3 in AUG selection. Using *in vivo* cross-linking, we observed accumulation of TC and mRNA/eIF4G on 40S subunits and a 48S 'halfmer' in *prt1-1* cells. Genetic evidence suggests that 40S–60S subunit joining is not rate-limiting in the *prt1-1* mutant. Thus, eIF3b functions between 48S assembly and subunit joining to influence AUG recognition and reinitiation on *GCN4* mRNA. Other mutations that disrupt eIF2–eIF3 contacts in the multifactor complex (MFC) diminished 40S-bound TC, indicating that MFC formation enhances 43S assembly *in vivo*.

The EMBO Journal (2004) **23,** 1166–1177. doi:10.1038/sj.emboj.7600116; Published online 19 February 2004
Subject Categories: RNA; proteins
Keywords: eIF3; GCN4 translational control; multifactor complex (MFC); PRT1; yeast

Introduction

Initiation of protein synthesis begins with the recruitment of initiator methionyl tRNA (Met-tRNA$_i^{Met}$) in a ternary complex (TC) with eIF2 and GTP to the 40S subunit, to form the 43S preinitiation complex. This is followed by recruitment of mRNA, prebound to the cap-binding complex eIF4F and the poly(A)-binding protein, to form the 48S preinitiation complex. The 43S complex scans the mRNA and AUG recognition triggers GTP hydrolysis in the TC, after which the 60S subunit joins and translation elongation begins. Following ejection of eIF2·GDP, the bound GDP is replaced with GTP by the guanine nucleotide exchange factor eIF2B in order to regenerate TC (Hershey and Merrick, 2000; Hinnebusch, 2000).

Mammalian eIF3 binds to the 40S ribosome and stimulates the binding of both TC and mRNA to 40S subunits *in vitro* (Hershey and Merrick, 2000; Hinnebusch, 2000). Yeast eIF3, consisting of the five subunits eIF3a/TIF32, eIF3b/PRT1, eIF3c/NIP1, eIF3i/TIF34 and eIF3g/TIF35, can restore binding of Met-tRNA$_i^{Met}$ (Danaie *et al*, 1995; Phan *et al*, 1998) and mRNA (Phan *et al*, 2001) to 40S ribosomes in heat-inactivated extracts of the *prt1-1* (eIF3b) mutant. Thus, yeast eIF3 performs two key functions ascribed to the mammalian factor. The recruitment of TC to the 40S subunit is also stimulated by eIF1 and eIF1A *in vitro* (Hershey and Merrick, 2000; Algire *et al*, 2002; Majumdar *et al*, 2003); however, the relative importance of these factors and of eIF3 for 43S formation *in vivo* is unclear.

In yeast, translational control of *GCN4* mRNA is a sensitive *in vivo* indicator of the rate of TC binding to 40S ribosomes. *GCN4* translation is activated by amino-acid starvation through a mechanism involving four upstream open reading frames (uORFs 1–4) in *GCN4* mRNA. After translating uORF1, many 40S subunits remain attached to the mRNA and resume scanning; however, *GCN4* translation is normally repressed because all of these 40S ribosomes rebind the TC before reaching uORF4, translate uORF4, and dissociate from the mRNA. Starvation leads to phosphorylation of eIF2α by GCN2, converting eIF2 from a substrate to a competitive inhibitor of eIF2B and reducing the concentration of TC (Hinnebusch, 1996). This allows ~50% of the rescanning 40S ribosomes to rebind TC after bypassing uORF4 and reinitiate at *GCN4* instead. *gcn2*Δ mutants fail to induce *GCN4* in starved cells and have a Gcn$^-$ (general control nonderepressible) phenotype. Mutations in eIF2B that lower TC levels derepress *GCN4* under nonstarvation conditions. This Gcd$^-$ (general control derepressed) phenotype does not require eIF2α phosphorylation and can be recognized in *gcn2*Δ cells (Hinnebusch, 1996).

We recently described the first mutation in eIF1A with a Gcd$^-$ phenotype, a deletion of the C-terminal 45 residues of the protein (Olsen *et al*, 2003). Importantly, overexpression of TC from a high-copy (hc) plasmid containing the genes for eIF2α, -β and -γ and tRNA$_i^{Met}$ (hc TC) suppressed the Gcd$^-$ phenotype of this mutation. This showed that eIF1A is required for optimal TC binding to 40S subunits *in vivo* and implicated eIF1A in the reinitiation process on *GCN4* mRNA. Mutations in eIF3 that reduce TC binding to 40S subunits should also produce a Gcd$^-$ phenotype, but none has been isolated.

In yeast, the TC is associated with eIF3, eIF1 and eIF5 in a multifactor complex (MFC) that can exist free of 40S

*Corresponding author. Laboratory of Gene Regulation and Development, National Institute of Child Health and Human Development, NIH, Building 6A/Room B1A-13, Bethesda, MD 20892-2716, USA. Tel.: +1 301 496 4480; Fax: +1 301 496 6828; E-mail: ahinnebusch@nih.gov

Received: 6 November 2003; accepted: 13 January 2004; published online: 19 February 2004

ribosomes (Asano *et al*, 2000). eIF2 interacts indirectly with NIP1/eIF3c in a manner bridged by eIF5 and it also binds directly to the C-terminal domain (CTD) of TIF32/eIF3a (Asano *et al*, 2000, 2001; Valášek *et al*, 2002). The *tif5-7A* mutation in eIF5 disrupts the indirect contact between eIF2 and eIF3 and leads to temperature-sensitive (Ts^-) growth *in vivo* and diminished TC recruitment *in vitro* (Asano *et al*, 1999, 2000). Reducing the direct contact between eIF2 and eIF3 by overexpressing a truncated TIF32 protein lacking the eIF2β-binding domain (hc-*TIF32Δ6*) confers a slow-growth (Slg^-) phenotype that is partially suppressed by hc TC. Combining *tif5-7A* and hc-*TIF32Δ6* produces a synthetic growth defect (Valášek *et al*, 2002), suggesting that the independent contacts between eIF2 and eIF3 in the MFC have additive effects on TC recruitment. However, the *tif5-7A* hc-*TIF32Δ6* double mutant does not have a Gcd^- phenotype, neither does it show reduced binding of TC to 40S subunits in cell extracts (Valášek *et al*, 2002). Thus, it appears that a reduction in TC recruitment is not the rate-limiting defect conferred by disruption of the MFC in this strain.

In an effort to implicate eIF3 directly in TC recruitment *in vivo*, we examined the effect of *prt1-1* on the level of 43S complexes in mutant cells at the restrictive temperature. This mutation replaces Ser-518 with Phe, and does not affect eIF3 integrity (Phan *et al*, 2001). Surprisingly, we saw an accumulation of eIF2 on 40S subunits in extracts of heat-treated *prt1-1* cells, and confirmed this result using a new technique for cross-linking preinitiation complexes in living cells. Consistent with the idea that 43S assembly is not rate-limiting in the *prt1-1* mutant, its Ts^- phenotype was not suppressed by hc TC and we observed a strong Gcn^- phenotype that likely results from a delay in scanning by reinitiating ribosomes on *GCN4* mRNA. Interestingly, *prt1-1* also increases the probability of rejecting a non-AUG start codon, implicating eIF3 in AUG recognition. These findings fit well with the fact that an eIF3 ortholog is lacking in prokaryotes, where scanning does not occur and AUG recognition relies heavily on base-pairing between rRNA in the 30S subunit and mRNA.

Results

TC and mRNA binding to 40S subunits is not diminished in prt1-1 cells at the restrictive temperature

We asked whether incubating *prt1-1* cells at the restrictive temperature would reduce the amount of eIF2 associated with 40S subunits, as predicted from a defect in 40S binding by the TC. Incubating *prt1-1* cells for 20 min at 37°C produced a run-off of polysomes and accumulation of 80S monosomes (Figure 1A, right panel), indicating a severe reduction in translation initiation (Hartwell and McLaughlin, 1968). Substantial amounts of eIF3, eIF2, eIF1 and eIF5 (components of the MFC), and eIF1A were found in the fractions containing free 40S subunits in the wild-type (WT) extracts (Figure 1B, left panel). Unexpectedly, there was an even greater proportion of eIF2 subunits in the 40S fraction from *prt1-1* cells (Figure 1B, right panel), at odds with the previous finding that *prt1-1* impairs TC binding to 40S subunits in heat-treated extracts (Danaie *et al*, 1995; Phan *et al*, 1998).

Owing to this discrepancy, we considered the possibility that the results in Figure 1 were an artifact of extract preparation. The binding of MFC components to 40S subunits during sedimentation through sucrose gradients requires heparin in the extraction buffer (Asano *et al*, 2000), and it was possible that heparin suppressed a defect in eIF2 binding in the *prt1-1* extract. To address this possibility, we developed a protocol for cross-linking 43S–48S complexes *in vivo* by formaldehyde (HCHO) treatment of living cells that eliminated the need for heparin. Cyclohexamide is also omitted because the cross-linking prevents polysome run-off in the extracts (data not shown).

Substantial proportions of eIF2, eIF3 and eIF1A cosedimented with the free 40S subunits in the whole-cell extracts (WCEs) from cross-linked WT cells (Figure 2B, left panel),

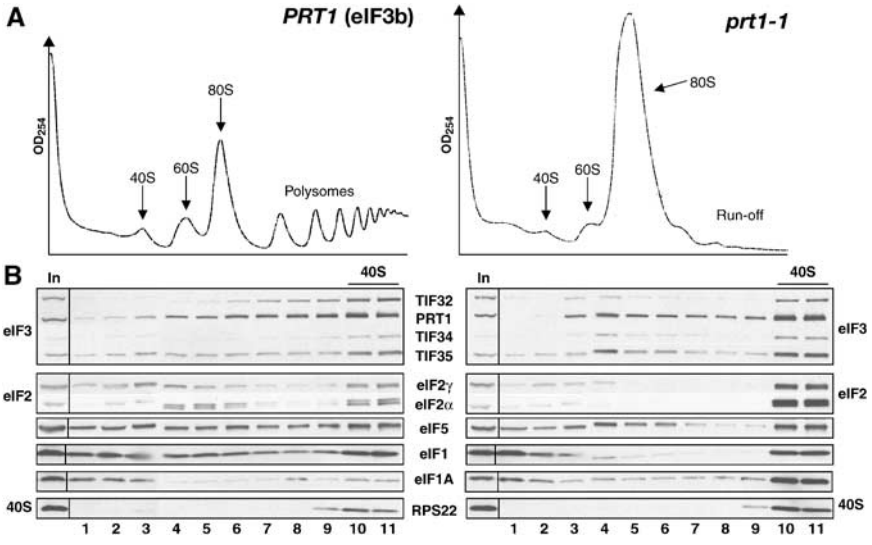

Figure 1 eIF2 remains bound to 40S subunits in extracts of *prt1-1* cells incubated at the nonpermissive temperature. (**A**) Isogenic *PRT1* (H2879) and *prt1-1* (H1676) cells were grown in YPD medium at 25°C and treated for 20 min at 37°C. Cyclohexamide was added to 50 μg/ml just prior to harvesting and WCEs prepared with heparin (200 μg/ml) in the breaking buffer were separated on a 4.5–45% sucrose gradient by centrifugation at 39 000 r.p.m. for 2.5 h. The gradients were collected and scanned at 254 nm to visualize the ribosomal species. (**B**) WCEs described in (A) were separated on a 7.5–30% sucrose gradient by centrifugation at 41 000 r.p.m. for 5 h. Proteins were subjected to Western analysis using antibodies against the proteins listed between the blots. An aliquot of each WCE was analyzed in parallel (In, input).

although smaller proportions of 40S-bound eIF5 and eIF1 were observed compared to the conventional protocol (Figure 1B). A significant proportion of eIF4G also cosedimented with 40S subunits (Figure 2B, left panel), whereas this factor is undetectable in the 40S fraction of WCEs prepared with heparin (data not shown). Total RNA was extracted from each fraction and probed for Met-tRNA$_i^{Met}$ and *RPL41A* mRNA by Northern analysis. The short length of this mRNA, 340 nt, ensures that free mRNP complexes sediment more slowly than 40S subunits. As expected, both tRNA$_i^{Met}$ and *RPL41A* mRNA peaked in the 40S fraction of cross-linked WT cells (Figure 2C, left panel).

Comparison of equivalent A_{260} units of WCEs from HCHO-treated WT and *prt1-1* cells revealed the expected reduction in polysomes and accumulation of 80S monosomes in the mutant cells incubated at 37°C (Figure 2A). Interestingly, the 40S fraction from the *prt1-1* cells had similar levels of eIF3, eIF5 and eIF1, and relatively greater amounts of eIF2, eIF4G, eIF1A, tRNA$_i^{Met}$ and mRNA compared to that seen in WT (Figure 2B and C). Quantification of the results from several experiments revealed that the amounts of 40S-bound eIF2γ, tRNA$_i^{Met}$ and mRNA were increased in the *prt1-1* cells by 166±58, 180±10 and 250±60%, respectively. The amount of free 40S subunits was generally greater in the mutant cells due to polysome run-off. If we normalize the amounts of 40S-bound eIF2, tRNA$_i^{Met}$ and mRNA for the RPS22 signals, then the levels of these 40S-bound factors are nearly identical between *prt1-1* and WT cells. However, because it is unknown whether 40S subunits are limiting for 43S/48S formation, we chose to compare the absolute levels of 40S-bound factors determined in replicate experiments. Regardless of how the data are quantified, the results indicate that 40S binding of TC, mRNA and eIF4G is not diminished in *prt1-1* cells at 37°C. We also found that similar amounts of eIF2 and eIF4G were present in the 80S and polysome fractions of WT and *prt1-1* mutant cells at 37°C, representing ~50% of the total pools of these factors, despite the low polysome content of the mutant at 37°C (data not shown). Thus, high levels of eIF2 and eIF4G are associated with both free and polysome-associated 48S complexes in the mutant. We conclude that the rate-limiting defect occurs at a step following assembly of 48S complexes in *prt1-1* cells at 37°C.

To validate the cross-linking technique, we wished to show that mutations in eIF2 would reduce the 40S binding of tRNA$_i^{Met}$ in cross-linked cells. Hence, we constructed a strain harboring a temperature-sensitive degron allele, *sui3-td*, encoding a fusion protein containing ubiquitin and a thermolabile dihydrofolate reductase moiety attached to the N-terminus of eIF2β, and expressed from a copper-dependent promoter. The strain also expresses the ubiquitin ligase UBR1 from a galactose-inducible promoter. Shifting the *sui3-td* cells from medium containing copper and raffinose at 25°C to medium containing galactose and lacking copper at 36°C represses new synthesis of the degron-tagged protein

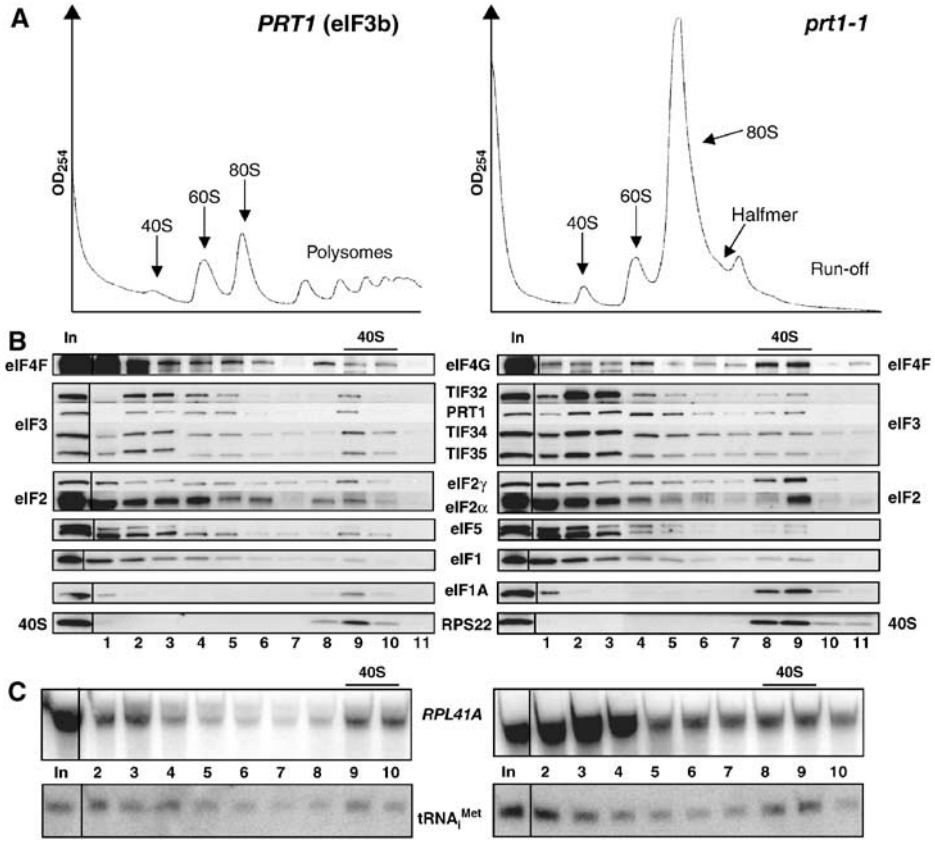

Figure 2 TC and mRNA remain bound to 40S subunits in HCHO-treated *prt1-1* cells at the nonpermissive temperature. *PRT1* (H2879) and *prt1-1* (H1676) cells were grown in YPD at 25°C, heat-treated for 20 min at 37°C, and cross-linked with HCHO for 15 min (**A**) or 1 h (**B**, **C**). (A) WCEs were separated and analyzed as in Figure 1A. (B, C) WCEs were separated and treated as in Figure 1B, except that each fraction was divided and analyzed by Western and Northern blotting.

(eIF2β^{td}), and the pre-existing eIF2β^{td} is rapidly eliminated by proteosomal degradation (Dohmen *et al*, 1994; Labib *et al*, 2000). After incubating under the nonpermissive condition for 16 h to deplete eIF2β^{td}, the *sui3-td* cells were treated with HCHO to cross-link the 43–48S complexes.

As expected, we observed polysome run-off in the cross-linked *sui3-td* cells under the nonpermissive condition (Figure 3A). Furthermore, eIF2β^{td} was undetectable and little or no eIF2γ and eIF2α cosedimented with free 40S subunits (Figure 3B, right panel). Importantly, the amount of tRNA$_i^{Met}$ in the 40S fraction (Figure 3C, right panel) declined to 14±4% of that seen under permissive conditions. There was little reduction in 40S binding of eIF3 subunits, and a small increase in 40S-bound eIF1A under the nonpermissive condition (Figure 3B), indicating a specific loss of TC from preinitiation complexes. We also examined the effects of a nonconditional mutation in eIF2γ, *gcd11-506*, which reduces the affinity of eIF2 for Met-tRNA$_i^{Met}$ *in vitro* (Erickson and Hannig, 1996). Consistently, we observed a threefold reduction in the amount of eIF2 on 40S subunits in cross-linked *gcd11-506* cells compared to WT (data not shown).

We next examined the *cdc33-1* mutant to examine the consequences of depleting the cap-binding protein, eIF4E, on mRNA recruitment. Incubating these cells at 37°C for 2 h leads to the disappearance of eIF4E, presumably due to proteolytic degradation (Figure 3D). The amount of 40S-bound mRNA also declined in the *cdc33-1* cells at 37°C to 47±8% of the level observed in WT cells, while the level of tRNA$_i^{Met}$ was reduced to only 86±10% of WT (Figure 3E). The ability of eIF4G to interact with both poly(A)-binding protein and eIF4E (Sachs, 2000) likely accounts for the residual mRNA binding to 40S ribosomes in *cdc33-1* cells at 37°C. As expected, we saw little reduction in the amounts of eIF3 or eIF2 subunits bound to free 40S subunits in the

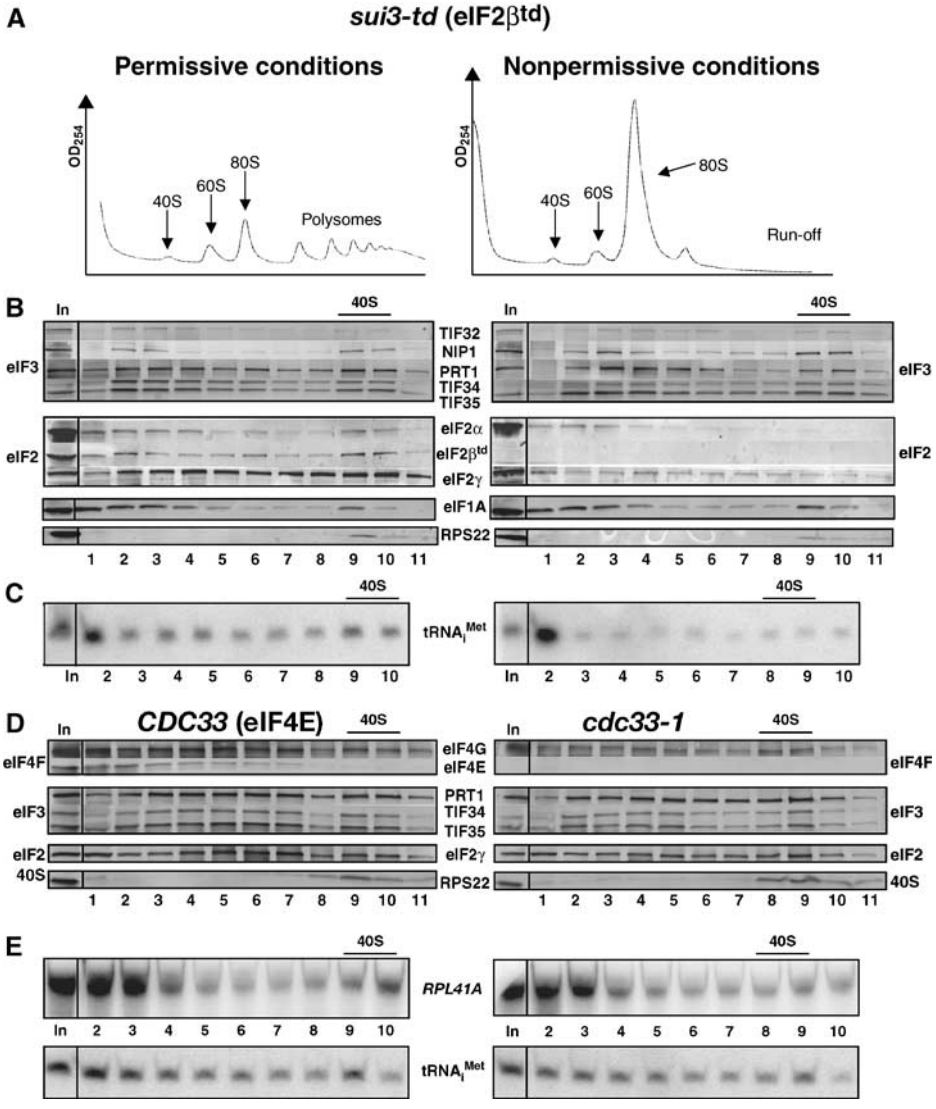

Figure 3 *sui3-td* and *cdc33-1* mutations reduce the binding of TC and mRNA to 40S subunits *in vivo*. (**A–C**) *sui3-td* (YAJ18-3) cells were grown in SC-raffinose in the presence of 0.1 M copper sulfate at 25°C and shifted to SC-raffinose + galactose in the absence of copper and grown overnight at 37°C. Cells were cross-linked with HCHO and analyzed as described in Figure 2A–C, except that eIF2β^{td} was detected in (B) using HA antibody. (**D**) Strain F324 was transformed with YEplac195-*CDC33-URA3* (*CDC33*) or empty vector (*cdc33-1*) and the resulting transformants were grown in SC-Ura medium at 25°C, heat treated for 2 h at 37°C, and cross-linked with HCHO. WCEs were prepared and analyzed as (B–C).

cdc33-1 mutant (Figures 3D). Thus, it appears that HCHO cross-linking provides a faithful depiction of the composition of preinitiation complexes in living cells.

If the rate-limiting defect in *prt1-1* cells is downstream from 48S complex assembly, we would expect to observe a halfmer shoulder on the 80S monosome formed by mRNAs containing an elongating 80S ribosome plus a 48S complex in the mRNA leader. As most monosomes in this mutant are 80S couples lacking mRNA (data not shown), the concentration of such $1\frac{1}{2}$-mers should be small. Nevertheless, we consistently detected a halfmer on the 80S peak in cross-linked *prt1-1* cells incubated for 20 min or 1 h at 37°C (Figure 4B and data not shown). In some experiments, the $1\frac{1}{2}$-mer was less prominent (Figure 2A, right panel), possibly due to the shorter HCHO treatment in those cases; however, we never detected a $1\frac{1}{2}$-mer peak in *cdc33-1* (Figure 4D) or *sui3-td* cells (Figure 3A, right panel). (We attribute the absence of the halfmer peak in Figure 1A to the presence of heparin, which could compete with mRNA for 40S binding.)

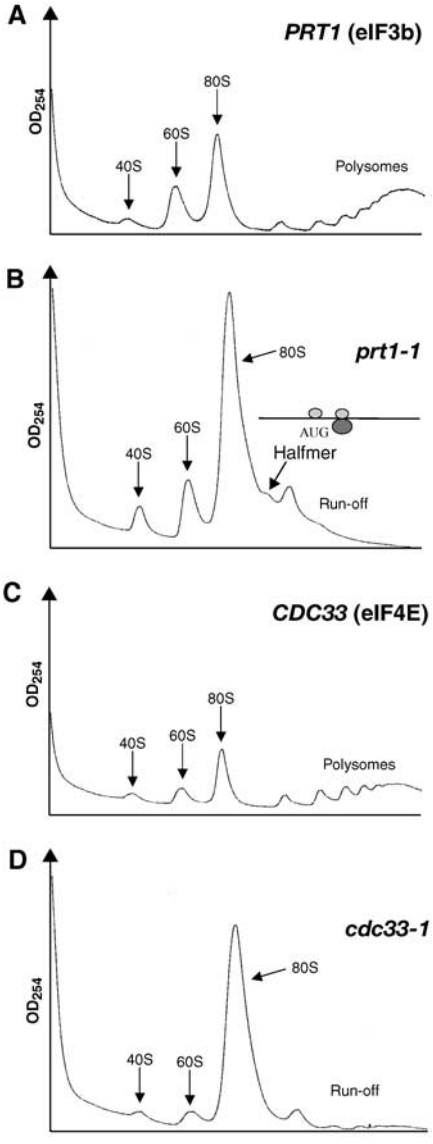

Figure 4 The *prt1-1* mutant displays a halfmer phenotype at the nonpermissive temperature. Polysome profiles of (**A**) *PRT1* (H2879) and (**B**) *prt1-1* (H1676) cells after 20 min at 37°C. The halfmer shoulder on the 80S peak is indicated along with an explanatory schematic of a $1\frac{1}{2}$-mer (see text). Polysome profiles of the (**C**) *CDC33* and (**D**) *cdc33-1* transformants described in Figure 3D after 2 h at 37°C.

Genetic evidence that TC binding to 40S subunits is not rate-limiting in prt1-1 cells

If binding of TC to 40S ribosomes was the principal deficiency in the *prt1-1* mutant, then its growth defect should be reduced by overexpressing TC from an hc plasmid. As expected, hc TC suppressed the growth defect of a *gcd1-502* mutant containing a defective subunit of eIF2B (Figure 5A, right panels) (Dever *et al*, 1995). By contrast, the growth defect of *prt1-1* cells at a semipermissive temperature of 33°C was not suppressed by hc TC (Figure 5A, left panels).

If *prt1-1* lowers the rate of TC binding to 40S subunits, then it should confer a Gcd$^-$ phenotype. Gcd$^-$ mutations suppress the sensitivity of *gcn2*Δ cells to 3-aminotriazole (3-AT), an inhibitor of the *HIS3* product, because they derepress *GCN4* translation, with attendant derepression of *HIS3*, independently of eIF2α phosphorylation by GCN2. We found that *prt1-1 gcn2*Δ cells displayed a weak Gcd$^-$ phenotype, allowing slightly better growth on 3-AT plates at 33°C compared to *PRT1 gcn2*Δ cells (Figure 5B, rows 2 and 3). This weak Gcd$^-$ phenotype was not suppressed by hc TC, however (Figure 5B, rows 1 and 2), suggesting that it does not result from impaired TC recruitment.

Unexpectedly, *prt1-1* cells containing GCN2 are sensitive to 3-AT (3-AT^s) at 33°C (Figure 5C, rows 2 and 4), the phenotype characteristic of Gcn$^-$ mutants. Consistently, derepression of a *GCN4–lacZ* reporter containing all four uORFs was conditionally defective in the *prt1-1 GCN2* cells, showing nearly WT induction by 3-AT at 25°C, but no induction at 33°C (Figure 6A, rows 2–4, 28 versus 30 U). Compared to the *PRT1 gcn2*Δ strain, *GCN4–lacZ* was partially derepressed under noninducing conditions at 33°C in the *prt1-1 GCN2* mutant (weak Gcd$^-$ phenotype) but did not increase further upon 3-AT induction. At 34°C, we observed only the strong Gcn$^-$ phenotype in the *prt1-1 GCN2* strain (Figure 6A, row 4, 7 versus 6 U), suggesting that it reflects the most severe defect produced by *prt1-1*.

The Gcn$^-$ phenotype of *prt1-1* cells could arise from a defect in eIF2α phosphorylation by GCN2. Western analysis using antibodies specific for eIF2α phosphorylated on Ser-51 (eIF2α-P) revealed an ~40% reduction in the level of eIF2α-P in the *prt1-1* mutant grown at 34°C with 10 mM 3-AT. Introducing *GCN2* on an hc plasmid into the *prt1-1* strain restored eIF2α-P to levels greater than or equal to those seen in the *PRT1* strain (data not shown), but derepression of *GCN4–lacZ* expression remained impaired (Figure 6A, row 1). Hence, the partial reduction in eIF2α phosphorylation in the *prt1-1* strain cannot account for its strong Gcn$^-$ phenotype.

It was possible that the reduced rate of translation initiation in *prt1-1* cells at 34°C would diminish the consumption of TC and restore TC to high levels even when eIF2α is phosphorylated. To test this, we asked whether a Ts$^-$ mutation in elongation factor eEF3 (encoded by *YEF3*) would produce a Gcn$^-$ phenotype at a semipermissive temperature (35°C) where the doubling time of the *yef3* mutant (~20 h) is similar to that of *prt1-1* cells at 34°C. The *yef3* mutant showed no Gcn$^-$ phenotype at 35°C (Figure 6A, row 5), making it

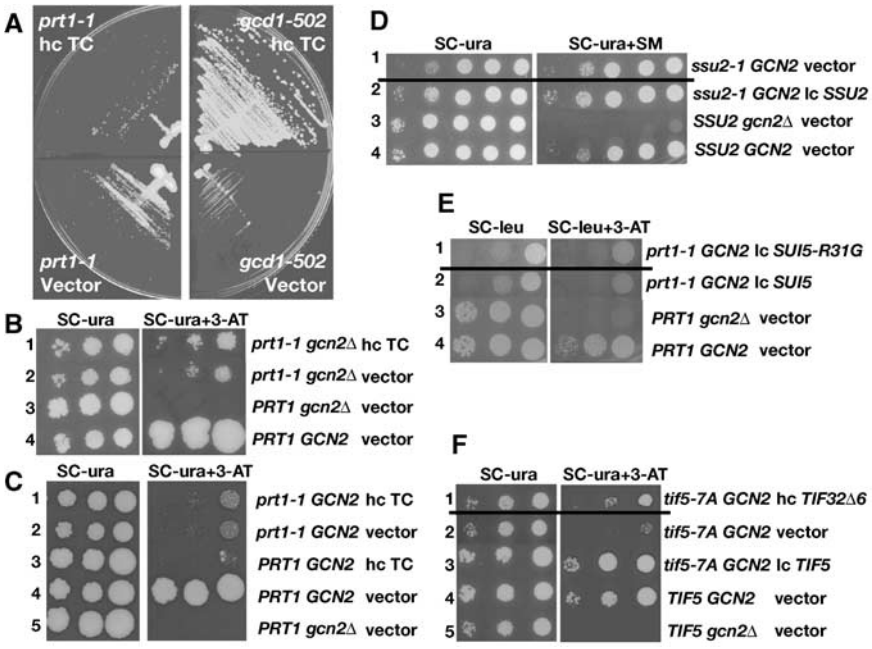

Figure 5 The *prt1-1* strain has a strong Gcn$^-$ phenotype and its Ts$^-$ phenotype is not suppressed by TC overexpression. (**A**) *prt1-1* (H1676) and *gcd1-502* (H70) cells were transformed with hc plasmid p3000 encoding hc TC, or empty vector, streaked on SC-Ura plates and incubated for 4 (left panels) or 2 days (right panels) at 33°C. (**B**) *prt1-1* (YKHN60) cells were transformed with p3000 (hc TC) or empty vector, grown overnight in SC-Ura, and 10-fold serial dilutions were spotted in rows 1 and 2 on SC-Ura plates or SC-Ura-His plates containing 40 mM leucine with 30 mM 3-AT and incubated for 7 and 10 days, respectively, at 33°C. *PRT1 GCN2* (H2879) and *PRT1 gcn2*Δ (H2881) cells transformed with empty vector were analyzed in parallel in rows 3 and 4. (**C**) *PRT1* (H2879) and *prt1-1* (H1676) cells were transformed with p3000 (hc TC) or empty vector and analyzed essentially as in (B). (**D**) *ssu2-1* (F708) cells were transformed with empty vector or p3342 encoding *SSU2* (*TIF5*), and analyzed in rows 1 and 2 as in (B), except using SC-Ura and SC-Ura-Ile-Val + 1 μg/μl SM plates and incubating for 2 or 3 days (row 1) and 1 or 2 days (rows 2–4) at 30°C. *SSU2 gcn2*Δ (H2881) and *SSU2 GCN2* (H2879) cells, transformed with empty vector, were analyzed in parallel in rows 3 and 4. (**E**) *prt1-1* (H1676) cells were transformed with p3993 encoding *SUI5-R31G* or p3992 encoding *SUI5* (*TIF5*) and analyzed essentially as in (B), except using SC-Leu plates or SC-Leu-His plates containing 10 mM 3-AT and incubating for 5 (row 1) or 3 days (row 2) at 33°C. *PRT1 gcn2*Δ (H2881) and *PRT1 GCN2* (H2879) cells, transformed with empty vector, were analyzed in parallel in rows 3 and 4, incubating for 2 days. (**F**) *tif5-7A GCN2* (YKHN206) cells were transformed with p3927 encoding *TIF32*Δ*6–His* or empty vector or p3342 encoding *TIF5* and analyzed essentially as in (B), except that plates were incubated at 30°C for 2 or 3 days (rows 2–5) and 3 or 4 days (row 1) due to the synthetic growth defect of the *tif5-7A TIF32*Δ*6–His* strain. *TIF5 GCN2* (YKHN205) and *TIF5 gcn2*Δ (H2898), transformed with empty vector, were analyzed in parallel in rows 4 and 5 and incubated for 2 or 3 days.

improbable that the Gcn$^-$ phenotype of *prt1-1* cells results from a reduced rate of translation.

A third possibility to explain the Gcn$^-$ phenotype of *prt1-1* cells would be if 40S subunits cannot resume scanning following translation of uORF1, as only rescanning subunits can bypass uORFs 2–4 and reinitiate at *GCN4* (Mueller and Hinnebusch, 1986). For example, 40S subunits might dissociate from the mRNA at the uORF1 stop codon or while scanning downstream from uORF1. To address this possibility, we examined a *GCN4–lacZ* construct containing only uORF1 and lacking the segment containing uORFs 2–4, (pM199). Expression of this construct is constitutively high in WT cells because a large proportion of ribosomes that translate uORF1 can resume scanning and reinitiate at *GCN4* regardless of TC levels (Grant *et al*, 1994). As shown in Figure 6B (row 2), there was no significant difference in the expression of this construct between *prt1-1* and *PRT1* cells in the presence of 3-AT. Hence, the proportion of ribosomes able to resume scanning and reach *GCN4* following uORF1 translation was unaltered by *prt1-1*. The same result was obtained for a construct containing solitary uORF1 at its natural distance from *GCN4* (data not shown).

The fourth mechanism we addressed was the possibility that ribosomes leaky scan uORF1 in *prt1-1* cells, making it impossible for them to bypass the remaining uORFs and reinitiate at *GCN4*. To test this possibility, we analyzed a *GCN4–lacZ* construct in which uORF1 is elongated and overlaps the beginning of *GCN4*. This elongated version of uORF1 blocks 98–99% of all scanning ribosomes from reaching the *GCN4* start site, indicating that only 1–2% of ribosomes leaky scan uORF1 in WT cells (Grant *et al*, 1994). We observed little or no increase in *GCN4–lacZ* expression from this construct under 3-AT-inducing conditions in *prt1-1* cells (Figure 6B, row 3). We also observed no increase in leaky scanning past uORF4 by assaying a construct containing solitary uORF4 at its normal location (Figure 6B, row 4). The results in rows 2–4 additionally eliminate the possibility that induction of *GCN4–lacZ* is reduced in *prt1-1* cells by a reduction in reporter mRNA level, as this effect should apply equally to the mutant constructs containing solitary uORFs 1 or 4, yet expression of these constructs was unaffected by *prt1-1*.

The fact that eliminating uORFs 2–4 completely suppresses the inability of *prt1-1* cells to induce *GCN4* expression (Figure 6B) provides strong genetic evidence that the Gcn$^-$ phenotype results from the inability of rescanning ribosomes to bypass uORFs 2–4 under starvation conditions when eIF2 is highly phosphorylated (Mueller and Hinnebusch, 1986). We envision two ways in which this could occur: (i) a reduction in the rate of scanning or (ii) a delay in GTP hydrolysis by 48S complexes at the start codons of uORFs

A

Units of β-galactosidase

	Genotype	*PRT1 GCN2*		*prt1-1 GCN2*		*prt1-1 hcGCN2*	
	3-AT	–	+	–	+	–	+
1	34ûC	65 ±10	300 ±21	21 ±5	24 ±4	22 ±7	19 ±0
2	25ûC	14 ±3	140 ±18	9 ±1	58 ±7		
3	33ûC	12 ±1	140 ±35	28 ±1	30 ±2		
4	34ûC	16 ±4	220 ±26	7 ±2	6 ±2		
	Genotype	*YEF3*		*yef3 ts*			
	SM	–	+	–	+		
5	35ûC	17 ±1	400 ±5	22 ±1	410 ±49		

B

Units of β-galactosidase

	Genotype	*PRT1 GCN2*		*prt1-1 GCN2*	
	3-AT	–	+	–	+
1	34ûC	16 ±4	220 ±26	7 ±2	6 ±2
2		290 ±9	400 ±45	560 ±160	530 ±130
3		8 ±1	15 ±2	19 ±2	19 ±5
4		20 ±3	39 ±3	32 ±3	32 ±1

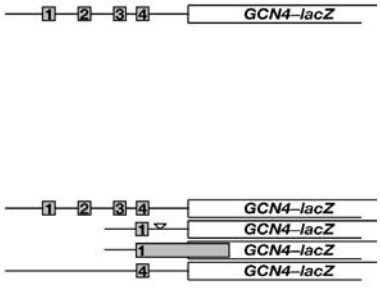

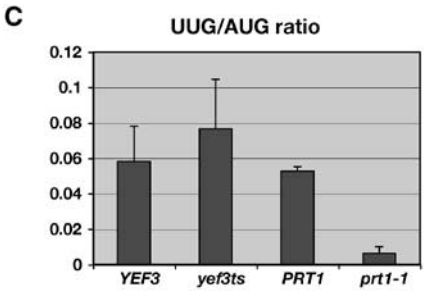

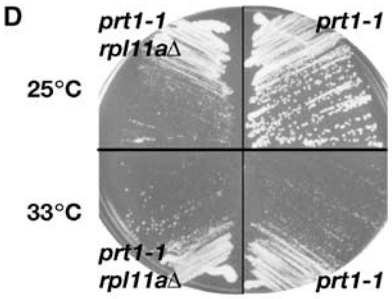

Figure 6 The *prt1-1* mutation impairs *GCN4* translational control, leads to hyperaccurate start codon selection, and does not show a synthetic growth defect with depletion of 60S subunit protein RPL11A. (**A**) *prt1-1* (H1676), *PRT1* (H2879), *YEF3* (F1006) or *yef3* (F650S) (F1007) cells were transformed with p180 containing the *GCN4–lacZ* fusion with all four uORFs and grown in SC-Ura in the presence or absence of 10 mM 3-AT, or 0.06 μg/μl SM, as shown, at the indicated temperatures. In row 1, the *prt1-1* strain was also transformed with hc *LEU2* plasmid (p832) containing *GCN2* (*hcGCN2*) or empty vector, and the *PRT1* strain also harbored an empty vector. β-Galactosidase activities were measured in WCEs and expressed in units of nmol of *o*-nitrophenyl-β-D-galactopyranoside hydrolyzed per min per mg of protein. The mean activities and standard errors obtained from independent transformants are indicated. (**B**) The *prt1-1* (H1676) and *PRT1* (H2879) strains were transformed with plasmids p180, pM199, pM226 or p226 (rows 1–4), respectively, and contained the *GCN4–lacZ* constructs shown schematically to the right and analyzed as in (A). Row 1 contains the same data as in row 4 of (A) shown for comparison. (**C**) *prt1-1* (H1676), *PRT1* (H2879), *YEF3* (F1006) or *yef3* ts (F1007) cells were transformed with p367 or p391 containing a *HIS4–lacZ* reporter harboring AUG or UUG start codons, respectively. The *PRT1* and *prt1-1* transformants were grown at 34°C, while the *YEF3* and *yef3 ts* transformants were grown at 35°C, in SC-Ura medium, and β-galactosidase was assayed in WCEs. The graph shows the mean ratios of expression from the UUG to the AUG reporter measured for four independent transformants of each strain (for each reporter), with standard errors indicated as error bars. (**D**) Growth of *prt1-1* (H1676) and *prt1-1 rpl11a*Δ (H2925) strains in YPD medium for 3 days at 25°C (upper panel) or 4 days at 33°C (lower panel).

2–4, creating a barrier to movement of all 40S subunits through the leader to *GCN4*. Either defect would increase the time required for 40S subunits lacking TC to scan past uORFs 2–4 and thereby compensate for the reduced rate of TC binding that results from eIF2α phosphorylation.

If a delay in GTP hydrolysis was responsible for the Gcn$^-$ defect in *prt1-1* cells, then the 3-AT^S phenotype should be reduced by expressing eIF5–G31R (encoded by *SUI5-R31G*), as eIF5–G31R has greater than WT activity in stimulating GTP hydrolysis by 40S-bound TC *in vitro* (Huang *et al*, 1997). However, *SUI5-R31G* did not alter the 3-AT^S phenotype of *prt1-1* even though it reduced the growth rate in nonstarvation medium when introduced into the *prt1-1* strain on a low-copy (lc) plasmid (Figure 5E, rows 1 and 2). (To compensate for its Slg$^-$ phenotype, the *prt1-1* lc*SUI5-R31G* strain was incubated 2 days longer than the *prt1-1* lc*SUI5* control strain.) We also asked whether the recessive Ts$^-$ *ssu2-1* mutation in eIF5, shown to impair GAP activity *in vitro* (Asano *et al*, 2001), would mimic *prt1-1* and confer a Gcn$^-$ phenotype. As shown in Figure 5D (rows 1 and 2), this was not the case, even though this mutation confers an Slg$^-$ phenotype. Thus, alterations in the GAP function of eIF5 do not impair the regulation of *GCN4* translation, pointing to a delay in scanning as the more likely explanation for the Gcn$^-$ phenotype of *prt1-1* cells.

The *tif5-7A* mutation in eIF5, which disrupts the connection between eIF2 and eIF3 in the MFC (Asano *et al*, 2000), does not affect GAP function *in vitro*, and we argued previously that it impairs the scanning process as the rate-limiting defect *in vivo* (Asano *et al*, 2001). Interestingly, *tif5-7A* shows a moderate Gcn$^-$ phenotype (Figure 5F, rows 2 and 3), consistent with the idea that optimal scanning is dependent on MFC integrity. Furthermore, the Gcn$^-$ phenotype of *tif5-7A* is suppressed by overexpressing the truncated eIF3a subunit TIF32-Δ6–His (Figure 5F, rows 1 and 2). As shown below, overexpressing TIF32-Δ6–His impairs TC binding to 40S subunits in *tif5-7A* cells. Hence, we propose that a scanning delay conferred by *tif5-7A* is compensated by the reduced TC binding produced by hc-*TIF32-Δ6–His*, restoring efficient *GCN4* induction in the double mutant.

The stringency of AUG recognition is altered in prt1-1 cells

To investigate the possibility that *prt1-1* alters the stringency of AUG selection during scanning, we measured the expression of *HIS4–lacZ* reporters containing either UUG or AUG as

a start codon. Interestingly, the selection of UUG was dramatically reduced in the mutant at 34°C, as the ratio of expression from the UUG versus AUG reporters (UUG/AUG ratio) was lower by a factor of 8–9 in *prt1-1* versus WT cells (Figure 6C). By contrast, the *yef3* Ts$^-$ mutation had little or no effect on the UUG/AUG ratio at a semipermissive temperature of 35°C. Northern analysis confirmed that the *HIS4–lacZ* mRNAs containing UUG or AUG were present at similar levels in *prt1-1* cells at 34°C (data not shown).

Evidence that subunit joining is not the rate-limiting defect in prt1-1 cells

Following hydrolysis of GTP by the TC, joining of the 60S subunit produces the 80S initiation complex in a reaction stimulated by eIF5B, encoded by *FUN12*. We wished to determine whether *prt1-1* impairs this final step in the pathway. Deletion of *FUN12* causes a strong Slg$^-$ phenotype (doubling time (T_d) of 5 versus 2 h for WT). The *rpl11a*Δ mutant, lacking one of two genes encoding 60S ribosomal protein RPL11, exhibits reduced subunit joining and an Slg$^-$ phenotype ($T_d = 3$ h) resulting from a decreased amount of 60S subunits (Rotenberg *et al*, 1988). Combining *fun12*Δ and *rpl11A*Δ leads to a synthetic growth defect ($T_d = 8$ h), consistent with an additive impairment of subunit joining in the double mutant. By contrast, the *prt1-1 rpl11a*Δ double mutant grows faster than the single *prt1-1* mutant at semipermissive temperature (Figure 6D), with doubling times of 15 and 22 h for the *prt1-1 rpl11a*Δ and *prt1-1* mutants, respectively, at 34°C. These results are inconsistent with the idea that the *prt1-1* mutant has a rate-limiting defect in 40S–60S subunit joining.

Biochemical evidence from in vivo cross-linking that eIF2–eIF3 contacts in the MFC enhance TC recruitment in vivo

We showed previously that overexpressing TIF32-Δ6–His leads to the formation of a defective MFC lacking eIF2, due to loss of the TIF32–CTD/eIF2β interaction (Valášek *et al*, 2002). The *tif5-7A* mutation in eIF5 disrupts the indirect contact between eIF2β and eIF3c/NIP1 (see the schematic in Figure 7B). Combining *tif5-7A* and hc-*TIF32-Δ6–His* produces a synthetic reduction in translation initiation and growth rate (Asano *et al*, 1999; Valášek *et al*, 2002). Although we expected to observe a reduction in TC binding to 40S subunits in the *tif5-7A* hc-*TIF32-Δ6–His* double mutant, this was not observed in WCEs prepared with heparin (Valášek *et al*, 2002). Hence, we used *in vivo* cross-linking to re-examine this prediction here.

As expected (Valášek *et al*, 2003), TIF32-Δ6–His did not bind to 40S ribosomes in *tif5-7A* cells and was located at the top of the gradient (Figure 7C). The eIF2γ and eIF3 subunits were present in the 40S fraction of the hc-*TIF32-Δ6–His tif5-7A* mutant (Figure 7A and C); however, quantification of four replicate experiments showed a reduction to 43 ± 8% of WT in the proportion of eIF2 in the 40S fraction, plus an increased proportion of unbound eIF2 at the top of the gradient (Figure 7D). The eIF3 subunits also showed a redistribution from the 40S-bound to unbound fractions and a decreased proportion in the MFC in the mutant cells (Figure 7D). These results indicate that destabilizing the MFC reduces TC recruitment *in vivo*. Our ability to detect a reduced level of 40S-bound eIF2 in the slow-growing *tif5-7A* hc-*TIF32-Δ6–His* cells, but not in the growth-arrested *prt1-1* cells at 37°C, underscores our conclusion that *prt1-1* impairs a critical postassembly function of eIF3. The fact that the reduction in TC binding is not greater than ~60% in *tif5-7A* hc-*TIF32-Δ6–His* cells, despite the marked reduction of polysomes (Valášek *et al*, 2002), is likely due to the fact that impaired TC binding is not the only defect in this double mutant.

Discussion

Yeast eIF3 has a critical function downstream of 48S assembly

The *prt1-1* (eIF3b) mutant shows a severe defect in 40S binding by Met-tRNA$_i^{Met}$ in heat-treated extracts (Danaie *et al*, 1995; Phan *et al*, 1998). However, we observed greater than WT amounts of eIF2 and tRNA$_i^{Met}$ associated with 40S subunits in *prt1-1* cells at the nonpermissive temperature, despite nearly complete inhibition of initiation (Figure 2A–C). Consistently, overexpression of TC did not reduce the Ts$^-$ phenotype of *prt1-1* cells at a semipermissive growth temperature (Figure 5A). We also observed an accumulation of eIF4G and *RPL41A* mRNA bound to 40S subunits (Figure 2B and C) and the appearance of a 48S halfmer on the 80S peak in *prt1-1* cells at 37°C. Thus, we conclude that the rate-limiting defect in the *prt1-1* mutant lies downstream of 48S assembly. We presented genetic evidence that 40S–60S subunit joining is not the rate-limiting defect in *prt1-1* cells by showing that *prt1-1* did not exacerbate the subunit joining defect in *rpl11a*Δ cells produced by a low level of 60S subunits. Together, our findings place the rate-limiting defect in *prt1-1* cells at one or more steps between 48S assembly and subunit joining, which include scanning, AUG recognition or GTP hydrolysis by the TC.

Our data do not necessarily indicate that binding of TC and mRNA to 40S subunits occurs at WT rates in *prt1-1* cells at 37°C. If *prt1-1* has a greater effect on conversion of 48S to 80S complexes than on 48S formation, there will be a net accumulation of 48S complexes at 37°C, as we observed. It is worth noting that endogenous eIF3, eIF2, eIF1 and eIF5 were found dissociated from 40S ribosomes when *prt1-1* extracts were heat treated at 37°C (Phan *et al*, 2001). Thus, the *prt1-1* product may be fully inactivated *in vitro*, but only partially impaired *in vivo*, producing a strong defect in 48S assembly only in extracts.

Our finding that *prt1-1* cells are more accurate than WT in selecting AUG versus UUG as the start codon, a hyperaccurate initiation (Hai$^-$) phenotype (Figure 6C), implicates eIF3 in AUG selection. A higher rate of eIF5-stimulated GTP hydrolysis by the TC increases the utilization of a near-cognate start codon (Sui$^-$ phenotype) (Huang *et al*, 1997). Thus, the Hai$^-$ phenotype of *prt1-1* mutant could result from a delay in GTP hydrolysis, although we discounted this defect as an explanation for its Gcn$^-$ phenotype. A reduced rate of scanning might indirectly affect AUG selection, but it is difficult to predict whether it would favor or disfavor the use of near-cognate codons. A third possibility is that *prt1-1* could destabilize Met-tRNA$_i^{Met}$ base-paired to near-cognate start codons in the P-site.

Mutations that impair TC recruitment confer a Gcd$^-$ phenotype by allowing ribosomes to scan past uORFs 2–4 and reinitiate at *GCN4* in the absence of eIF2α phosphorylation. A C-terminal truncation of eIF1A has a Gcd$^-$ phenotype that can be suppressed by hc TC, providing evidence that eIF1A stimulates 43S complex formation *in vivo* (Olsen *et al*, 2003).

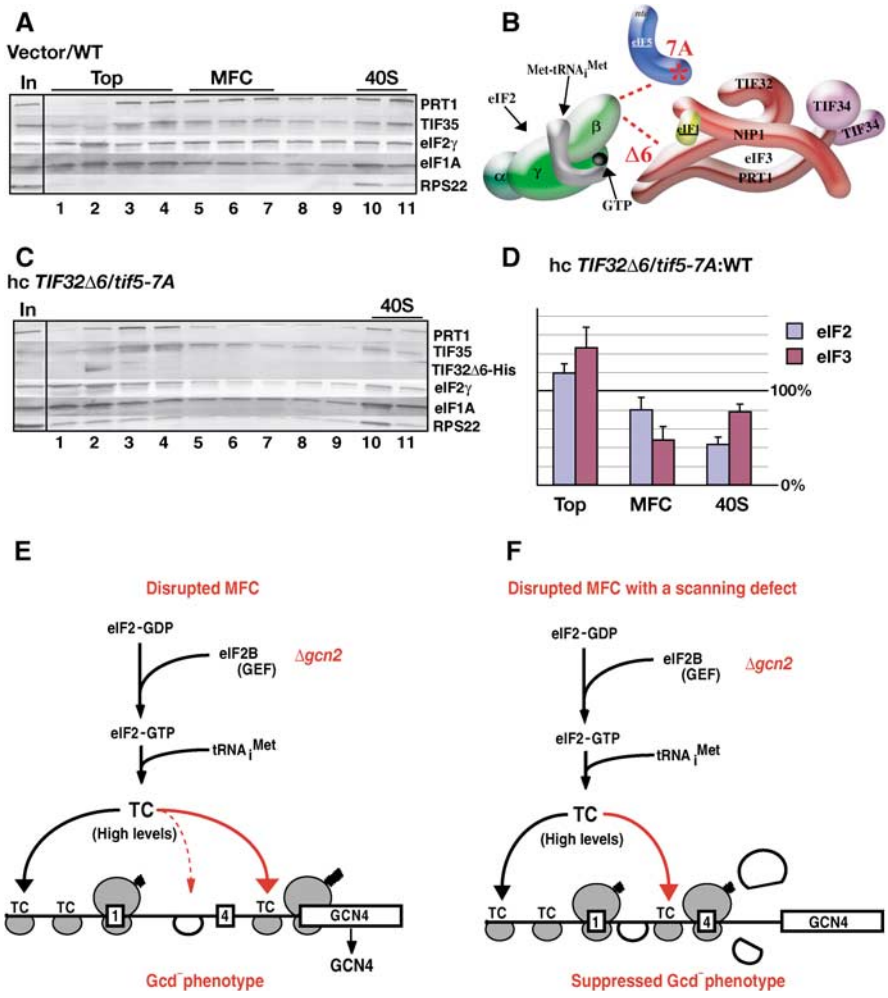

Figure 7 Redistribution of eIF2 from the 40S-bound to the 40S-free state in the hc-*TIF32*Δ*6 tif5-7A* mutant (**A**–**D**) and schematic model to explain the differing effects of mutations in MFC components on *GCN4* translational control (**E**). (A) WT strain H2898 transformed with empty vector and (C) *tif5-7A* strain H2899 transformed with hc plasmid p3927 containing *TIF32*Δ*6–His* were grown in SC-Ura medium and cross-linked with HCHO. WCEs were separated and analyzed as in Figure 2B. (B) Schematic representation of the defective MFC in hc-*TIF32*Δ*6 tif5-7A* cells lacking the contact between eIF2β and TIF32–CTD and that between eIF2β and NIP1–NTD bridged by eIF5 (see text). (D) The amounts of eIF2γ (eIF2) or PRT1 (eIF3) in fractions 1–4 (top), 5–7 (MFC), and 10–11 (40S) were quantified with a PhosphorImager or by videodensitometry using NIH image 1.63 software, and the resulting values for the hc-*TIF32*Δ*6 tif5-7A* strain were normalized to the corresponding WT values. The results from four independent experiments were averaged and the mean normalized values and standard errors were plotted, with 100% corresponding to the WT values. The assignment of the MFC to fractions 5–7 was based on our previous analysis of mutant MFC complexes (Valášek *et al*, 2003). (E) Mutations in MFC components (*prt1-1*, *TIF32*Δ*6* or *tif5-7A*) that decrease the rate of TC binding to 40S subunits scanning downstream from uORF1 should allow a fraction of 40S subunits to bypass uORF4 and reinitiate at *GCN4*, even in the absence of eIF2α phosphorylation in *gcn2*Δ cells where TC levels are high (Gcd$^-$ phenotype). (**F**) The rate-limiting defects conferred by mutations in MFC components reduce the rate of scanning by 40S subunits following uORF1 translation. This compensates for the reduced rate of TC recruitment caused by these mutations and thereby suppresses the Gcd$^-$ phenotype predicted from the recruitment defects.

By contrast, the *prt1-1* mutant does not show a Gcd$^-$ phenotype that is suppressible by hc TC (Figure 5B); moreover, it fails to induce *GCN4* translation when eIF2α is phosphorylated under starvation conditions (Figures 5C and 6A)—a strong Gcn$^-$ phenotype. As removal of uORFs 2–4 overcomes the effect of *prt1-1* on *GCN4* translation, we can attribute the Gcn$^-$ phenotype to the failure of any 40S ribosomes rescanning after uORF1 translation to bypass uORFs 2–4 when TC levels are reduced by eIF2α phosphorylation (Mueller and Hinnebusch, 1986). Interestingly, deletion of eIF5B leads to a strong Gcn$^-$ phenotype that arises partly from an increase in leaky scanning past uORF1 (Choi *et al*, 1998; Lee *et al*, 2002; Shin *et al*, 2002). We ruled out this possibility for *prt1-1*, indicating distinct mechanisms for the Gcn$^-$ phenotypes of *fun12*Δ and *prt1-1* mutants.

The simplest way to explain the Gcn$^-$ phenotype of *prt1-1* cells is to propose a decrease in the rate of scanning. This would compensate for the reduced rate of TC binding produced by eIF2α phosphorylation and ensure that all 40S subunits will rebind TC before reaching uORF4 (Figure 7E and F). This would be equivalent to increasing the distance between uORFs 1 and 4, which also produces a Gcn$^-$ phenotype (Abastado *et al*, 1991). An alternative possibility would be that the fraction of rescanning ribosomes which rebind TC in the uORF1–uORF4 interval become stalled at AUG codons 2, 3 or 4 by a defect in GTP hydrolysis. This would produce a roadblock at these uORFs and increase the time required for all free 40S ribosomes to reach uORF4. This latter mechanism is disfavored by our finding that expressing eIF5–R31G, shown to have hyperactive GAP function (Huang

et al, 1997), did not diminish the Gcn$^-$ phenotype of *prt1-1* cells (Figure 5E). Moreover, a mutant containing the GAP-defective eIF5–G62S protein (Asano *et al*, 2001) does not exhibit a Gcn$^-$ phenotype (Figure 5D). On the other hand, the *tif5-7A* allele, whose product shows WT GAP function (Asano *et al*, 2001), does confer a moderate Gcn$^-$ phenotype (Figure 5F) and we presented evidence consistent with defective scanning in this strain (Asano *et al*, 2001). Thus, we favor the model that the Gcn$^-$ phenotype of *prt1-1* results from a defect in scanning rather than impaired GTP hydrolysis by eIF2. There is evidence that eIF1 is required for efficient scanning by a 48S complex *in vitro* (Pestova *et al*, 1998); hence, *prt1-1* could impair scanning indirectly by impeding eIF1 function. Indeed, *prt1-1* weakens the association between the eIF3/eIF5 subcomplex and eIF1 (Phan *et al*, 2001).

Integrity of the MFC is required for optimal TC recruitment in vivo

Our previous genetic data led us to conclude that the direct eIF2β–TIF32 contact in the MFC disrupted by hc-*TIF32-Δ6* and the indirect eIF2β–NIP1 contact eliminated by *tif5-7A* have additive stimulatory effects on TC recruitment (Valášek *et al*, 2002). However, we were unable to detect a reduction in eIF2 binding to 40S subunits in heparin-stabilized extracts. Here, using HCHO cross-linking, we consistently observed an ~60% reduction in eIF2 binding to 40S subunits in the hc-*TIF32-Δ6 tif5-7A* double mutant (Figure 7C and D). We have also confirmed by *in vivo* cross-linking that TC binding to 40S subunits is not significantly impaired in the *tif5-7A* single mutant (data not shown). These data provide the first biochemical evidence that disrupting multiple contacts between eIF2 and eIF3 in the MFC reduces TC recruitment *in vivo*.

Despite the reduced TC recruitment in the hc-*TIF32-Δ6 tif5-7A* mutant, this strain does not show a Gcd$^-$ phenotype (Valášek *et al*, 2002). The solution to this paradox may be provided by our finding that the *tif5-7A* single mutant has a Gcn$^-$ phenotype, which is suppressed by overexpressing TIF32-Δ6–His (Figure 5F). Thus, the reduced rate of scanning conferred by *tif5-7A* could compensate for the diminished TC binding that results from TIF32-Δ6–His overexpression. This would restore efficient reinitiation at uORFs 2–4 and suppress the Gcd$^-$ phenotype expected from defective TC recruitment (Valášek *et al*, 2002) (Figure 7E and F). Presumably, *prt1-1* confers a Gcn$^-$ phenotype because it has a relatively stronger effect on scanning and a minimal impact on TC binding.

Concluding remarks

Our combined genetic and biochemical analysis of the *prt1-1* mutant has allowed us to demonstrate that eIF3 has critical functions downstream of the 48S complex assembly and prior to 60S subunit joining, which impact ribosomal scanning on *GCN4* mRNA and AUG selection. Similarly, the results described here and elsewhere (Asano *et al*, 2001; Valášek *et al*, 2002) indicate that disrupting contacts between eIF3 and eIF2 in the MFC reduces the rate of TC recruitment *in vivo* and also impairs postassembly functions of the 48S complex involved in *GCN4* control. Several key results supporting these conclusions were obtained using HCHO cross-linking of live cells to fix native initiation complexes. This new technique obviates the use of stabilizing compounds that alter the composition or abundance of 48S complexes, and it was shown previously that HCHO cross-linking also prevents artifactual 43S formation in cell extracts (Kumar *et al*, 1989). The experiments we conducted to validate this technique gave interesting results in their own right, which deserve further exploration. These include the fact that eIF1A and eIF3 bind to 40S subunits independently of eIF2, that the affinity of eIF2 for the 40S subunit is promoted by interaction with Met-tRNA$_i^{Met}$, and that high-level binding of eIF4G to 40S subunits can occur in the absence of eIF4E *in vivo*.

The Gcn$^-$ phenotypes of *prt1-1* and *tif5-7A* mutants provide the first evidence that both eIF3 activity and MFC integrity are required for the specialized reinitiation mechanism underlying *GCN4* translational control. It now seems likely that eIF3 and eIF5 must rebind to the 40S subunits following uORF1 translation to insure the proper rate of scanning from uORF1 to uORFs 2–4. This in turn dictates the fraction of 40S subunits that do not rebind TC before reaching uORF4 and thus go on to reinitiate at *GCN4* instead. It is possible that translation of *GCN4*, or other mRNAs similarly controlled by uORFs, will be modulated by signaling pathways that target eIF3 function or assembly of the MFC.

Materials and methods

Yeast strains and plasmids

Strains and plasmids used in this study are listed in Tables 1 and 2, respectively, and details of their construction are provided in the Supplementary Materials.

HCHO cross-linking, WCE preparation and fractionation of extracts for analysis of preinitiation complexes

WCE extracts were made from 200 ml of cells grown to an OD_{600} of ~1.5 in YPD or SC medium. Cells were transferred to a 500 ml centrifuge tube containing 50 g of shaved ice and the tube was inverted five times. HCHO was added to 1% and the tube was inverted 10 times and left on ice for 1 h. Glycine was added to 0.1 M and the cells were collected by centrifugation for 5 min at 7000 r.p.m. in a Sorvall RC5B rotor. The pellet was resuspended in 10 ml of buffer B (20 mM Tris (pH 7.5), 50 mM KCl, 10 mM $MgCl_2$) supplemented with EDTA-free protease inhibitor tablet (Roche), 5 mM NaF, 1 mM dithiothreitol, 1 mM phenylmethylsulfonylfluoride (PMSF) and 1 μg/ml of the following protease inhibitors–pepstatin A, aprotenin and leupeptin. For Northern analysis, 0.2 μg/ml of diethyl pyrocarbonate was also added. The cell suspension was transferred to a 15 ml conical tube and centrifugated for 5 min at 4200 r.p.m. in a Beckman J-6B centrifuge and the supernatant was decanted. One vol of cells was resuspended in ~1.3 vol of buffer B and 1.3 vol of glass beads, and cells were lysed by vortexing eight times for 30 s with 30 s intervals on ice. The lysate was centrifugated for 5 min at 4200 r.p.m. and the supernatant was transferred to an Eppendorf tube. The extract was cleared by two consecutive centrifugations at 13 000 r.p.m. for 5 and 10 min in an Eppendorf 5415D centrifuge, collecting the supernatant while avoiding the lipid layer at the top and the pellet. The WCEs were separated by sedimentation through sucrose gradients as described previously (Asano *et al*, 2000). For Western analysis, the fractions were precipitated with 1 ml of 100% ethanol at −20°C overnight. Boiling of the samples in SDS-loading buffer for 10 min was sufficient to reverse the cross-linking. RNA was extracted from the fractions essentially as described (Cigan *et al*, 1991), except that the RNA was extracted twice with hot (70°C) phenol for 15 min, which was sufficient to reverse the cross-linking.

Other biochemical methods

Please refer to Supplementary Materials.

Supplementary data

Supplementary data are available at *The EMBO Journal* Online.

Table I *S. cerevisiae* strains used in this study

Strain	Genotype	Source or reference
H1676[a]	*MATa prt1-1 leu2-3,112 ura3-52*	Phan *et al* (1998)
H2879[a]	*MATa PRT1 leu2-3,112 ura3-52*	This study
H2880[a]	*MATa trp1Δ leu2-3,112 ura3-52*	This study
H2881[a]	*MATa trp1Δ leu2-3,112 ura3-52 gcn2::hisG*	This study
YAJ18-3[a]	H2881 sui3::cup1p-ubi-DHFR^{ts}-HA-sui3^{td}-URA3 ubr1::Gal1-10p-mycUBR1-TRP1	This study
YKHN60[a]	*MATa trp1Δ leu2-3,112 ura3-52 gcn2::hisG prt1::hisG pKHN7[prt1-1 LEU2]*	This study
H2925[a]	*MATa prt1-1 leu2-3,112 ura3-52 rpl11aΔ*	This study
H2926[a]	*MATa PRT1 leu2-3,112 ura3-52 rpl11aΔ*	This study
F324	*MATα cdc33 leu1 ura3 trp1 ade8*	K Matsumoto
H2898[b]	*MATa ura3-52 leu2-3 leu2-112 trp1-Δ63 gcn2Δ tif5Δ::hisG tif34Δ::hisG* p[TIF5-FL TRP1] p[TIF34-HA LEU2]	Asano *et al* (2000)
H2899 [b]	*MATa ura3-52 leu2-3 leu2-112 trp1- Δ63 gcn2Δ tif5Δ::hisG tif34Δ::hisG* p[tif5-7A-FL TRP1] p[TIF34-HA LEU2]	Asano *et al* (2000)
YKHN205[b]	*MATa ura3-52 leu2-3 leu2-112 trp1-Δ63 GCN2$^+$ tif5Δ::hisG tif34Δ::hisG* p[TIF5-FL TRP1] p[TIF34-HA LEU2]	This study
YKHN206[b]	*MATa ura3-52 leu2-3 leu2-112 trp1- Δ63 GCN2$^+$ tif5Δ::hisG tif34Δ::hisG* p[tif5-7A-FL TRP1] p[TIF34-HA LEU2]	This study
H70	*MATα his1-29 gcn2-101 gcn3-101 ura3-52 gcd1-502 (HIS4-lacZ, ura3-52)*	Harashima and Hinnebusch (1986)
F1006[c]	*MATa ura3-52 leu2-3, 112 trp1-7 lys2 met2-1 his4-713 yef3::LEU2* p*[YEF3 TRP1]*	Anand *et al* (2003)
F1007[c]	*MATa ura3-52 leu2-3, 112 trp1-7 lys2 met2-1 his4-713 yef3::LEU2* p*[yef3-F650S TRP1]*	Anand *et al* (2003)
J115[d]	*MATα ura3-52 leu2-3,112 fun12Δ p[FUN12 URA3]*(pC479)	Lee *et al* (2002)
J116F[d]	*MATα ura3-52 leu2-3,112 fun12Δ*	Lee *et al* (2002)
J113[d]	*MATα ura3-52 leu2-3,112 fun12Δ rpl11aΔ p[FUN12 URA3]*(pC479)	Lee *et al* (2002)
J113F[d]	*MATα ura3-52 leu2-3,112 fun12Δ rpl11aΔ*	Lee *et al* (2002)
F708	*MATa ura3-52 his4- tif5-G62S*	T Donahue

[a]Isogenic strains.
[b]Isogenic strains.
[c]Isogenic strains.
[d]Isogenic strains.

Table II Plasmids used in this study

Name	Description	Source or reference
YEplac195–CDC33 (B3351)	High copy vector expressing *CDC33*	Cruz *et al* (1997)
YEp24–hc TC (B3000)	High copy URA3 vector expressing *SUI2*, *SUI3*, *GCD11* and *IMT4*	Asano *et al* (1999)
Yep13–GCN2 (B832)	High copy LEU2 vector expressing *GCN2*	Ramirez *et al* (1991)
YCp50–GCN4–lacZ (B180)	Low copy URA3 vector containing wild-type GCN4 leader	Mueller and Hinnebusch (1986)
pM199	Low copy URA3 vector containing only uORF1 at uORF4s position	Grant *et al* (1994)
pM226	Derived from pM199; ORF of uORF1 extends into *GCN4* sequence	Grant *et al* (1994)
Ycp50–GCN4–lacZ (B226)	Low copy URA3 vector containing GCN4 leader with only uORF4	Mueller and Hinnebusch (1986)
YCp50–HIS4–AUG–lacZ	Low copy URA3 vector containing HIS4–AUG–lacZ fusion (p367)	Donahue and Cigan (1988)
YCp50–HIS4–AUU–lacZ	Low copy URA3 vector containing HIS4–AUU–lacZ fusion (p391)	Donahue and Cigan (1988)
YEplac–*TIF32-Δ6–His* (B3927)	High copy URA3 vector expressing *TIF32-Δ6–His*	Valášek *et al* (2002)
YCplac33–TIF5 (B3342)	Low copy URA3 vector expressing *TIF5*	Asano *et al* (1999)
pRS415 (B3992)	Low copy LEU2 vector expressing *SUI5 (TIF5)*	Huang *et al* (1997)
pRS415 (B3993)	Low copy LEU2 vector expressing *SUI5-R31G*	Huang *et al* (1997)

Acknowledgements

We thank Patrick Linder, Terry Kinzy and Tom Donahue for providing plasmids and yeast strains, Ernest Hannig for GCD11 antiserum, Tom Dever for suggestions and a critical reading of the manuscript, and members of the Hinnebusch and Dever laboratories for helpful discussions. BS received a PhD fellowship grant from the Bay Zoltan Foundation for Applied Research in Hungary.

References

Abastado JP, Miller PF, Jackson BM, Hinnebusch AG (1991) Suppression of ribosomal reinitiation at upstream open reading frames in amino acid-starved cells forms the basis for *GCN4* translational control. *Mol Cell Biol* **11:** 486–496

Algire MA, Maag D, Savio P, Acker MG, Tarun Jr SZ, Sachs AB, Asano K, Nielsen KH, Olsen DS, Phan L, Hinnebusch AG, Lorsch JR (2002) Development and characterization of a reconstituted yeast translation initiation system. *RNA* **8:** 382–397

Anand M, Chakraburtty K, Marton MJ, Hinnebusch AG, Kinzy TG (2003) Functional interactions between yeast translation eukaryotic elongation factor (eEF) 1A and eEF3. *J Biol Chem* **278:** 6985–6991

Asano K, Clayton J, Shalev A, Hinnebusch AG (2000) A multifactor complex of eukaryotic initiation factors eIF1, eIF2, eIF3, eIF5, and initiator tRNA^{Met} is an important translation initiation intermediate *in vivo*. *Genes Dev* **14:** 2534–2546

Asano K, Krishnamoorthy T, Phan L, Pavitt GD, Hinnebusch AG (1999) Conserved bipartite motifs in yeast eIF5 and eIF2Bε, GTPase-activating and GDP-GTP exchange factors in translation initiation, mediate binding to their common substrate eIF2. *EMBO J* **18:** 1673–1688

Asano K, Shalev A, Phan L, Nielsen K, Clayton J, Valášek L, Donahue TF, Hinnebusch AG (2001) Multiple roles for the carboxyl terminal domain of eIF5 in translation initiation complex assembly and GTPase activation. *EMBO J* **20:** 2326–2337

Choi SK, Lee JH, Zoll WL, Merrick WC, Dever TE (1998) Promotion of Met-tRNA$_i^{Met}$ binding to ribosomes by yIF2, a bacterial IF2 homolog in yeast. *Science* **280:** 1757–1760

Cigan AM, Foiani M, Hannig EM, Hinnebusch AG (1991) Complex formation by positive and negative translational regulators of *GCN4*. *Mol Cell Biol* **11:** 3217–3228

Danaie P, Wittmer B, Altmann M, Trachsel H (1995) Isolation of a protein complex containing translation initiation factor Prt1 from *Saccharomyces cerevisiae*. *J Biol Chem* **270:** 4288–4292

Dever TE, Yang W, ström S, Byström AS, Hinnebusch AG (1995) Modulation of tRNA$_i^{Met}$, eIF-2 and eIF-2B expression shows that *GCN4* translation is inversely coupled to the level of eIF-2.GTP.Met-tRNAiMet ternary complexes. *Mol Cell Biol* **15:** 6351–6363

Dohmen RJ, Wu P, Varshavsky A (1994) Heat-inducible degron: a method for constructing temperature-sensitive mutants. *Science* **263:** 1273–1276

Donahue TF, Cigan AM (1988) Genetic selection for mutations that reduce or abolish ribosomal recognition of the *HIS4* translational initiator region. *Mol Cell Biol* **8:** 2955–2963

Erickson FL, Hannig EM (1996) Ligand interactions with eukaryotic translation initiation factor 2: role of the γ-subunit. *EMBO J* **15:** 6311–6320

Grant CM, Miller PF, Hinnebusch AG (1994) Requirements for intercistronic distance and level of eIF-2 activity in reinitiation on GCN4 mRNA varies with the downstream cistron. *Mol Cell Biol* **14:** 2616–2628

Harashima S, Hinnebusch AG (1986) Multiple *GCD* genes required for repression of *GCN4*, a transcriptional activator of amino acid biosynthetic genes in *Saccharomyces cerevisiae*. *Mol Cell Biol* **6:** 3990–3998

Hartwell LH, McLaughlin CS (1968) Temperature-sensitive mutants of yeast exhibiting a rapid inhibition of protein synthesis. *J Bacteriol* **96:** 1664–1671

Hershey JWB, Merrick WC (2000) Pathway and mechanism of initiation of protein synthesis. In *Translational Control of Gene Expression*, Sonenberg N, Hershey JWB, Mathews MB (eds), pp 33–88. Cold Spring Harbor: Cold Spring Harbor Laboratory Press

Hinnebusch AG (1996) Translational control of *GCN4*: gene-specific regulation by phosphorylation of eIF2. In *Translational Control*, Hershey JWB, Mathews MB, Sonenberg N (eds), pp 199–244. Cold Spring Harbor, NewYork: Cold Spring Harbor Laboratory Press

Hinnebusch AG (2000) Mechanism and regulation of initiator methionyl-tRNA binding to ribosomes. In *Translational Control of Gene Expression*, Sonenberg N, Hershey JWB, Mathews MB (eds), pp 185–243. Cold Spring Harbor: Cold Spring Harbor Laboratory Press

Huang H, Yoon H, Hannig EM, Donahue TF (1997) GTP hydrolysis controls stringent selection of the AUG start codon during translation initiation in *Saccharomyces cerevisiae*. *Genes Dev* **11:** 2396–2413

Kumar RV, Wolfman A, Panniers R, Henshaw EC (1989) Mechanism of inhibition of polypeptide chain initiation in calcium-depleted Ehrlich ascites tumor cells. *J Cell Biol* **108:** 2107–2115

Labib K, Tercero JA, Diffley JF (2000) Uninterrupted MCM2-7 function required for DNA replication fork progression. *Science* **288:** 1643–1647

Lee JH, Pestova TV, Shin BS, Cao C, Choi SK, Dever TE (2002) Initiation factor eIF5B catalyzes second GTP-dependent step in eukaryotic translation initiation. *Proc Natl Acad Sci USA* **99:** 16689–16694

Majumdar R, Bandyopadhyay A, Maitra U (2003) Mammalian translation initiation factor eIF1 functions with eIF1A and eIF3 in the formation of a stable 40 S preinitiation complex. *J Biol Chem* **278:** 6580–6587

Mueller PP, Hinnebusch AG (1986) Multiple upstream AUG codons mediate translational control of *GCN4*. *Cell* **45:** 201–207

Olsen DS, Savner EM, Mathew A, Zhang F, Krishnamoorthy T, Phan L, Hinnebusch AG (2003) Domains of eIF1A that mediate binding to eIF2, eIF3 and eIF5B and promote ternary complex recruitment *in vivo*. *EMBO J* **22:** 193–204

Pestova TV, Borukhov SI, Hellen CUT (1998) Eukaryotic ribosomes require initiation factors 1 and 1A to locate initiation codons. *Nature* **394:** 854–859

Phan L, Schoenfeld LW, Valášek L, Nielsen KH, Hinnebusch AG (2001) A subcomplex of three eIF3 subunits binds eIF1 and eIF5 and stimulates ribosome binding of mRNA and tRNA$_i^{Met}$. *EMBO J* **20:** 2954–2965

Phan L, Zhang X, Asano K, Anderson J, Vornlocher HP, Greenberg JR, Qin J, Hinnebusch AG (1998) Identification of a translation initiation factor 3 (eIF3) core complex, conserved in yeast and mammals, that interacts with eIF5. *Mol Cell Biol* **18:** 4935–4946

Ramirez M, Wek RC, Hinnebusch AG (1991) Ribosome-association of GCN2 protein kinase, a translational activator of the *GCN4* gene of *Saccharomyces cerevisae*. *Mol Cell Biol* **11:** 3027–3036

Rotenberg MO, Moritz M, Woolford Jr JL (1988) Depletion of *Saccharomyces cerevisiae* ribosomal protein L16 causes a decrease in 60S ribosomal subunits and formation of half-mer polyribosomes. *Genes Dev* **2:** 160–172

Sachs A (2000) Physical and functional interactions between the mRNA cap structure and the poly(A) tail. In *Translational Control of Gene Expression*, Sonenberg N, Hershey JWB, Mathews MB (eds), pp 447–465. Cold Spring Harbor: Cold Spring Harbor Laboratory Press

Shin BS, Maag D, Roll-Mecak A, Arefin MS, Burley SK, Lorsch JR, Dever TE (2002) Uncoupling of initiation factor eIF5B/IF2 GTPase and translational activities by mutations that lower ribosome affinity. *Cell* **111:** 1015–1025

Valášek L, Mathew A, Shin BS, Nielsen KH, Szamecz B, Hinnebusch AG (2003) The yeast eIF3 subunits TIF32/a and NIP1/c and eIF5 make critical connections with the 40S ribosome *in vivo*. *Genes Dev* **17:** 786–799

Valášek L, Nielsen KH, Hinnebusch AG (2002) Direct eIF2–eIF3 contact in the multifactor complex is important for translation initiation *in vivo*. *EMBO J* **21:** 5886–5898